HHS Public Access

Author manuscript

Cell Rep. Author manuscript; available in PMC 2020 January 30.

Published in final edited form as:

Cell Rep. 2019 December 24; 29(13): 4583–4592.e3. doi:10.1016/j.celrep.2019.11.107.

Intracellular Vesicle Fusion Requires a Membrane-Destabilizing Peptide Located at the Juxtamembrane Region of the v-SNARE

Shailendra S. Rathore[1,4,5], **Yinghui Liu**[1,2,5], **Haijia Yu**[1,2,*], **Chun Wan**[1], **MyeongSeon Lee**[1], **Qian Yin**[3], **Michael H.B. Stowell**[1], **Jingshi Shen**[1,6,*]

[1]Department of Molecular, Cellular and Developmental Biology, University of Colorado, 347 UCB, Boulder, CO 80309, USA

[2]Jiangsu Key Laboratory for Molecular and Medical Biotechnology, College of Life Sciences, Nanjing Normal University, Nanjing 210023, China

[3]Department of Biological Sciences and Institute of Molecular Biophysics, Florida State University, Tallahassee, FL 32306, USA

[4]Present address: School of Applied and Engineering Physics, Cornell University, Ithaca, NY 14853, USA

[5]These authors contributed equally

[6]Lead Contact

SUMMARY

Intracellular vesicle fusion is mediated by soluble N-ethylmaleimide sensitive factor attachment protein receptors (SNAREs) and Sec1/Munc18 (SM) proteins. It is generally accepted that membrane fusion occurs when the vesicle and target membranes are brought into close proximity by SNAREs and SM proteins. In this work, we demonstrate that, for fusion to occur, membrane bilayers must be destabilized by a conserved membrane-embedded motif located at the juxtamembrane region of the vesicle-anchored v-SNARE. Comprised of basic and hydrophobic residues, the juxtamembrane motif perturbs the lipid bilayer structure and promotes SNARE-SM-mediated membrane fusion. The juxtamembrane motif can be functionally substituted with an unrelated membrane-disrupting peptide in the membrane fusion reaction. These findings establish the juxtamembrane motif of the v-SNARE as a membrane-destabilizing peptide. Requirement of membrane-destabilizing peptides is likely a common feature of biological membrane fusion.

Graphical Abstract

*Correspondence: haijiayu@gmail.com (H.Y.), jingshi.shen@colorado.edu (J.S.).

AUTHOR CONTRIBUTIONS

S.S.R., H.Y., and J.S. conceived the project. S.S.R., Y.L., H.Y., and C.W. performed the experiments. M.L. and Q.Y. contributed to structural modeling. S.S.R., H.Y., M.H.B.S., and J.S. wrote the manuscript with input from all authors.

SUPPLEMENTAL INFORMATION

Supplemental Information can be found online at https://doi.org/10.1016/j.celrep.2019.11.107.

DECLARATION OF INTERESTS

The authors declare no competing interests.

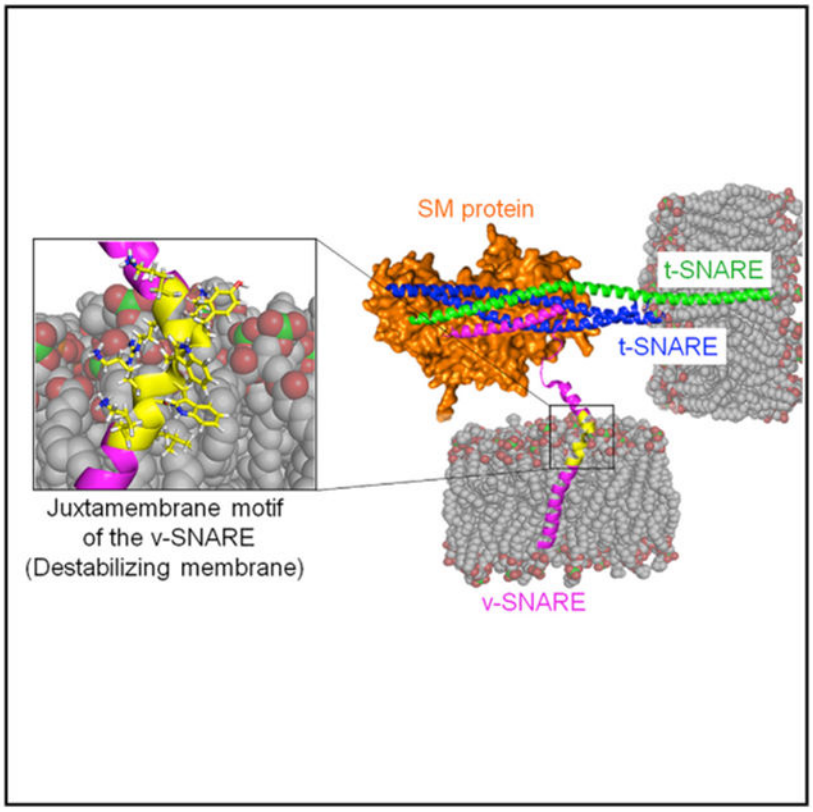

In Brief

Membrane fusion occurs when the vesicle and target membranes are brought into close proximity by SNAREs and SM proteins. In this work, Rathore et al. demonstrate that, for fusion to occur, membrane bilayers must be destabilized by a conserved membrane-embedded motif located at the juxtamembrane region of the vesicle-anchored v-SNARE.

INTRODUCTION

Membrane fusion—the merging of two lipid bilayers into one—involves substantial membrane remodeling and lipid rearrangements, imposing a high energy barrier that must be overcome by specialized membrane fusion proteins (Kozlov et al., 2010; Martens and McMahon, 2008; Südhof and Rothman, 2009). An extensively studied form of membrane fusion is the merging of intracellular vesicles with their target membranes, which transports cargo proteins between organelles in the endomembrane system (Baker and Hughson, 2016; Brunger et al., 2009; Ohya et al., 2009; Wickner, 2010). Intracellular vesicle fusion is driven by two conserved families of molecules: SNAREs (soluble N-ethylmaleimide sensitive factor attachment protein receptors) and SM (Sec1/Munc18) proteins (Rizo and Südhof, 2012; Shen et al., 2007). The vesicle-anchored v-SNARE pairs with the target membrane-associated t-SNAREs to form a four-helix *trans*-SNARE complex, forcing the two membranes into close apposition to fuse (Krämer and Ungermann, 2011; Schwartz and Merz, 2009; Söllner et al., 1993). A cognate SM protein activates SNARE zippering and

ensures SNARE pairing specificity (Baker et al., 2015; Ma et al., 2013; Shen et al., 2007; Yu et al., 2018).

Theoretical modeling suggests that, to overcome the energy barrier of membrane fusion, the lipid bilayer structure must be disrupted after the two membranes are brought into close proximity (Chernomordik and Kozlov, 2008; Kozlov et al., 2010; Risselada and Grubmüller, 2012). In viral fusion, another type of extensively studied membrane fusion, viral fusion proteins possess membrane-destabilizing peptides required for the fusion of enveloped viruses with host cell membranes (Earp et al., 2005; Harrison, 2008). Virus-anchored fusion proteins bring the viral limiting membrane and the host cell membrane (the plasma membrane or the endosome) into close apposition as they refold between the membrane bilayers, analogous to the role of the *trans*-SNARE complex in intracellular vesicle fusion (Chlanda et al., 2016; Harrison, 2008; Lamb and Jardetzky, 2007; Martens and McMahon, 2008; Top et al., 2005). Viral fusion proteins use fusion peptides to anchor the virus to the host cell (Harrison, 2008). Interestingly, in addition to their membrane-anchoring function, fusion peptides can directly destabilize lipid bilayers to promote viral membrane fusion (Düzgüneş and Shavnin, 1992; Earp et al., 2005; Epand, 2003; Haldar et al., 2018; Huang et al., 2004; Shmulevitz et al., 2004). Besides fusion peptides, the membrane-proximal external regions of viral fusion proteins can also destabilize membrane bilayers (Allison et al., 1999; Buzon et al., 2010; Howard et al., 2008; Jeetendra et al., 2003; Muñoz-Barroso et al., 1999; Vishwanathan and Hunter, 2008). More recently, membrane-destabilizing peptides were also discovered in non-viral fusion proteins such as atlastins, which drive homotypic endoplasmic reticulum (ER) fusion (Faust et al., 2015; Liu et al., 2012).

Membrane-destabilizing peptides have not been known to exist in the SNARE-SM vesicle fusion machinery, raising the possibility that intracellular vesicle fusion might proceed through a route distinct from other membrane fusion pathways. In this work, we discovered that the juxtamembrane motif of the v-SNARE directly perturbs the lipid bilayer structure in a manner reminiscent of viral fusion proteins. Mutations of the juxtamembrane motif abrogate SNARE-SM-mediated fusion *in vitro*, correlating with the essential role of the juxtamembrane motif in vesicle fusion in the cell. Importantly, the juxtamembrane motif can be functionally replaced by an unrelated membrane-disrupting peptide in membrane fusion. Thus, intracellular vesicle fusion also requires a membrane-destabilizing peptide, supporting the notion that membrane-destabilizing peptides constitute a universal element in membrane fusion reactions. These findings suggest that biological membrane fusion pathways, although driven by disparate fusion proteins, are governed by common underlying mechanisms.

RESULTS

The Juxtamembrane Motif of VAMP2 Is Required for SNARE-Munc18-1-Mediated Membrane Fusion

Membrane-destabilizing peptides in viral fusion and homotypic ER fusion are usually short segments embedded in the surface of lipid bilayers (Chernomordik and Kozlov, 2003; Earp et al., 2005; Liu et al., 2012). VAMP2/synaptobrevin, a v-SNARE involved in synaptic exocytosis (Martin et al., 2013; Söllner et al., 1993), possesses a conserved juxtamembrane

motif linking the force-generating SNARE motif to the transmembrane domain (Figure 1A; Bowen and Brunger, 2006; Brewer et al., 2011). Buried in the outer leaflet of the membrane bilayer, the juxtamembrane motif contains hydrophobic residues that insert into the nonpolar phase of the lipid bilayer as well as basic residues localized to the polar phase of the membrane (Figure 1B; Bowen and Brunger, 2006; Brewer et al., 2011; Ellena et al., 2009; Kweon et al., 2003). The juxtamembrane motif is critical for exocytosis *in vivo* (Borisovska et al.,2012; DeMill et al., 2014; Williams et al., 2009), but its role in the membrane fusion reaction has remained unclear.

To examine the function of the juxtamembrane motif in membrane fusion, synaptic exocytic SNAREs (syntaxin-1, SNAP-25, and VAMP2) and SM protein (Munc18-1) were reconstituted into a liposome fusion assay. The kinetics of the liposome fusion reactions were measured using lipid and content mixing assays (Yu et al., 2019). The conserved residues of the juxtamembrane motif were mutated into alanines, and the VAMP2 mutant was reconstituted into proteoliposomes at the same density as the wild-type (WT) protein (Figures 2A, 2B, and S1A). We observed that the SNARE-Muncl8-1-mediated fusion reaction was strongly inhibited when the juxtamembrane motif was mutated (Figures 2C–2E, S1B, and S2). In contrast, the basal SNARE-driven fusion (without Munc18-1) was not affected by the mutation (Figures 2C–2E and S2). The selective involvement of the juxtamembrane motif in the SNARE-Munc18-1-mediated fusion reaction is consistent with the discovery that basal SNARE-driven fusion is fundamentally distinct from the SM protein-assisted fusion pathway (Baker et al., 2015; Jiao et al., 2018; Yu et al., 2018). The SNARE-SM-mediated fusion reaction, but not basal SNARE-driven fusion, recapitulates intracellular vesicle fusion (Walter et al., 2010; Yu et al., 2015, 2018).

These results demonstrate that the juxtamembrane motif of VAMP2 is critical for SNARE-Munc18-1-mediated membrane fusion.

The Juxtamembrane Motif of VAMP2 Is Dispensable for SNARE-Munc18-1 Association

Next, we sought to define how the juxtamembrane motif of VAMP2 promotes membrane fusion at the molecular level. We first examined whether the juxtamembrane motif influences membrane docking. The t-SNARE liposomes were anchored to avidin beads and used to bind v-SNARE liposomes. Pairing of v- and t-SNAREs allowed the v-SNARE liposomes to dock onto the bead-anchored t-SNARE liposomes, which was moderately enhanced by Munc18-1 (Figure 3A). We observed that mutations of the VAMP2 juxtamembrane motif did not affect docking of the liposomes (Figure 3A). Hence, the juxtamembrane motif is not involved in the docking step of the membrane fusion reaction.

In a liposome co-flotation assay, WT and mutant VAMP2 bound equally well to the t-SNAREs (Figure S3). Thus, the juxtamembrane motif is dispensable for SNARE complex assembly, consistent with the ability of the VAMP2 mutant to drive normal basal fusion (Figures 2C and 2D). Next, we examined whether the juxtamembrane motif regulates SNARE-Munc18-1 association. Using isothermal titration calorimetry (ITC), we observed that the affinity of Munc18-1 binding to the WT SNARE complex was similar to its binding to the mutant SNARE complex in which the juxtamembrane motif of VAMP2 was mutated (Figure 3B). We then further examined SNARE-Munc18-1 binding using a glutathione S-

transferase (GST) pull-down assay. We observed that mutation of the juxtamembrane motif did not impair the interaction of GST-Munc18-1 with the SNARE complex (Figure 3C), in agreement with the ITC results. Thus, although selectively required for the SNARE-Munc18-1-mediated fusion reaction, the juxtamembrane motif of VAMP2 is dispensable for formation of the SNARE-Munc18-1 complex.

Together, these data demonstrate that the juxtamembrane motif of VAMP2 is dispensable for SNARE complex formation and SNARE-Munc18-1 association, supporting a model where it promotes membrane fusion through lipid binding.

The Function of the VAMP2 Juxtamembrane Motif Requires Both Basic and Hydrophobic Residues

The juxtamembrane motif of VAMP2 is comprised of basic and hydrophobic residues that directly interact with lipids (Figures 1B and 4A; Bowen and Brunger, 2006; Brewer et al., 2011; Ellena et al., 2009; Han et al., 2016). It has been speculated that electrostatic interactions between the basic residues and lipid head groups are involved in the vesicle fusion reaction (Montal, 1999; Williams et al., 2009). Direct evidence for this model, however, has been lacking. Next, we examined the functional role of a conserved stretch of basic residues (K85/R86/K87) in the juxtamembrane motif (Figure 4A). We observed that SNARE-Munc18-1-mediated liposome fusion was strongly inhibited when the K85/R86/K87 (KRK) stretch was deleted or mutated into alanines (Figure 4B), indicating a critical role of these residues in the fusion reaction. We reasoned that, if the KRK stretch promotes membrane fusion through electrostatic interactions with lipids, then its activity should rely on the overall charge rather than specific amino acids. To test this possibility, the KRK sequence was substituted with triple lysines (KKK) or triple arginines (RRR) (Figure 4A), both of which retained the overall charge of the juxtamembrane motif. Indeed, VAMP2 variants bearing the KKK or RRR substitutions were fully active in mediating SNARE-Munc18-1-mediated liposome fusion (Figure 4B). We then replaced the KRK sequence with six histidine residues (His_6), which are weakly basic at pH 7.4 (Figure 4A). We found that the VAMP2 variant bearing the His_6 substitution also supported SNARE-Munc18-1-mediated liposome fusion, albeit with a lower efficiency (Figure 4B), consistent with partial protonation of histidine side chains at neutral pH. By contrast, substitution of the KRK stretch with acidic residues (EDE) abrogated SNARE-Munc18-1-mediated liposome fusion (Figure 4B). None of these mutations significantly affected basal SNARE-driven fusion (Figure 4B), confirming the dispensability of the juxtamembrane motif in the basal fusion reaction. These data demonstrate that the function of the juxtamembrane motif in membrane fusion requires the basic residues.

The juxtamembrane motif of VAMP2 also contains a hydrophobic stretch (residues 88–93) buried in the nonpolar phase of the membrane bilayer (Bowen and Brunger, 2006; Kweon et al., 2003). We observed that SNARE-Munc18-1-mediated liposome fusion was strongly inhibited when this hydrophobic stretch was deleted or mutated into alanines (Figure 4B). Thus, like the basic residues, the hydrophobic stretch is critical for the function of the juxtamembrane motif in membrane fusion.

Together, these data demonstrate that both the basic and hydrophobic stretches are required for the function of the VAMP2 juxtamembrane motif in SNARE-Munc18-1-mediated membrane fusion. Because these regions are known to interact with lipids (Bowen and Brunger, 2006; Brewer et al., 2011; Ellena et al., 2009), our data further suggest that the juxtamembrane motif promotes membrane fusion by directly binding to the lipid bilayer.

The Juxtamembrane Motif of VAMP2 Destabilizes the Membrane Bilayer

Next, we sought to determine whether the juxtamembrane motif of VAMP2 directly influences the integrity of membrane bilayers. A synthetic peptide encompassing the VAMP2 juxtamembrane motif was added to protein-free liposomes (Figure 5A). Using a dequenching-based liposome leakage assay, we observed that the juxtamembrane motif peptide induced significant content release from the population of liposomes (Figures 5B and 5C). In contrast, peptides derived from other SNARE sequences, including the N-peptide of syntaxin-1 and the Vc peptide of VAMP2, did not induce content release (Figures 5B and 5C). Because membrane disruption is often accompanied by lipid mixing (Bailey et al., 1997; Thorén et al., 2005), we next examined whether the SNARE-derived peptides can induce liposome lipid mixing. Indeed, the juxtamembrane motif peptide, but not the N-peptide or Vc peptide, induced lipid mixing of protein-free liposomes (Figure S4), correlating with the membrane-disrupting activity of the juxtamembrane motif peptide (Figures 5B and 5C). Next, we used negative staining electron microscopy to visualize the effect of the juxtamembrane motif peptide on liposome morphology. We observed that protrusions emanated from liposomes incubated with the juxtamembrane motif peptide but not the N-peptide or Vc peptide (Figure 5D), consistent with the ability of the juxtamembrane motif peptide to remodel membrane bilayers.

Thus, the juxtamembrane motif of VAMP2 is intrinsically capable of disrupting the lipid bilayer structure. These data strongly suggest that the juxtamembrane motif of VAMP2 promotes SNARE-Munc18-1-mediated membrane fusion by destabilizing the membrane bilayer.

The Juxtamembrane Motif of VAMP2 Can Be Functionally Substituted with an Unrelated Membrane-Destabilizing Peptide

We reasoned that, if the juxtamembrane motif of VAMP2 promotes membrane fusion by destabilizing the lipid bilayer, then it could be functionally substituted with an unrelated peptide known to disrupt the membrane structure. To test this possibility, the VAMP2 juxtamembrane motif was replaced with the TatP59W peptide, a variant of the Tat peptide derived from the Tat protein of human immunodeficiency virus-1 (HIV-1) (Thorén et al., 2005). Like the VAMP2 juxtamembrane motif, the TatP59W peptide is a short membrane-embedded stretch comprised of both basic and hydrophobic residues (Figure 6A; Thorén et al., 2005). Importantly, the TatP59W peptide exhibits no sequence similarity with the juxtamembrane motif of VAMP2 and is not involved in exocytosis (Figure 6A; Thorén et al., 2005). We observed that, although mutations of the juxtamembrane motif abolished SNARE-Munc18-1 mediated liposome fusion, the fusion was restored when the TatP59W peptide was introduced into the juxtamembrane region of VAMP2 (Figure 6B). Thus, the juxtamembrane motif of VAMP2 can be replaced by an unrelated bilayer-disrupting peptide

in the membrane fusion reaction, further demonstrating that the juxtamembrane motif promotes membrane fusion by destabilizing the lipid bilayer.

Linker Insertions Diminish SNARE-Munc18-1-Mediated Membrane Fusion

In all v-SNAREs, the SNARE motif is directly connected to the juxtamembrane motif without extra residues between them (Figure 1A). Insertions of flexible linkers between the SNARE and juxtamembrane motifs of VAMP2 strongly inhibit exocytosis *in vivo* (Deák et al., 2006; DeMill et al., 2014; Kesavan et al., 2007). However, it was unclear whether and how the linker insertions directly influence the vesicle fusion reaction. Next, we introduced helix-breaking glycine and serine residues between the SNARE motif and juxtamembrane motif of VAMP2 (Figure 7A). We observed that these linker insertions had little effect on the basal SNARE-driven liposome fusion reaction (Figure 7B). Insertion of 21 residues only moderately reduced the basal SNARE-driven liposome fusion, whereas shorter insertions had no effect on the fusion kinetics (Figure 7B). We then examined how the linker insertions affect the SNARE-Munc18-1-mediated fusion reaction. We found that insertion of two residues resulted in normal fusion kinetics (Figure 7B). However, further extension of the linker strongly inhibited SNARE-Munc18-1-mediated liposome fusion (Figure 7B). With seven or more helix-disrupting residues added, the liposome fusion reaction was essentially reduced to the basal level (Figure 7B), similar to mutations of the juxtamembrane motif (Figures 2 and 4).

Thus, the SNARE-Munc18-1-mediated fusion reaction is highly sensitive to linker insertions, indicating that the membrane-destabilizing juxtamembrane motif must be directly connected to the force-generating SNARE motif with minimal spacing. Interestingly, *in vivo* exocytosis also tolerated a two-residue insertion but was abrogated when longer linkers were introduced (Figure 7C; Deák et al., 2006; Kesavan et al., 2007). The strong correlation of our biochemical data with genetic observations further supports the physiological relevance of the membrane-destabilizing function uncovered in this work.

DISCUSSION

Although the cytoplasmic domains of SNAREs and their interactions with SM proteins have been well characterized, little has been known about protein-membrane interactions in the vesicle fusion reaction. In this work, we discovered that the membrane-embedded juxtamembrane motif of VAMP2 promotes membrane fusion by destabilizing the lipid bilayer. This membrane-destabilizing function is supported by three lines of evidence: (1) mutations or deletions of the lipid-binding residues in the juxtamembrane motif inhibit SNARE-Munc18-1-mediated membrane fusion; (2) the juxtamembrane motif is intrinsically capable of disrupting lipid bilayer structures; and (3) an unrelated membrane-disrupting peptide can replace the juxtamembrane motif in promoting membrane fusion. Because the juxtamembrane motif is conserved among v-SNAREs, we anticipate that its membrane-destabilizing function is required for all vesicle fusion pathways. With the discovery of a membrane-destabilizing peptide in intracellular vesicle fusion, we suggest that biological membrane fusion pathways, although driven by disparate proteins, are governed by a common principle: assembly or refolding of membrane fusion proteins brings two lipid

bilayers into close proximity, followed by local disruption of the bilayer structure by membrane-destabilizing peptides.

How does the juxtamembrane motif of the v-SNARE destabilize the membrane bilayer? Electron microscopy (EM) imaging showed that the juxtamembrane motif deforms the membrane bilayer, which creates local elastic stresses and reduces the energy barrier for membrane merging (Kozlov et al., 2010; McMahon et al., 2010). Curvature induction usually requires the cooperative action of multiple copies of a membrane-binding molecule (Hui et al., 2009; McMahon et al., 2010) so that the juxtamembrane motif is unable to induce curvature within free v-SNAREs. When multiple SNARE complexes (three or more) zipper cooperatively in a vesicle fusion reaction (Domanska et al., 2009; Mohrmann et al., 2010; Shi et al., 2012), it is conceivable that their juxtamembrane motifs are concentrated at the fusion sites, allowing curvature induction. This curvature-inducing activity can be recapitulated by adding high concentrations of synthetic juxtamembrane motif peptides (Figure 5D). The juxtamembrane peptide of the v-SNARE may also promote dehydration of lipid head groups, which disrupts membrane integrity and neutralizes negative lipid charges to reduce the repulsive force of approaching membranes (Martens and McMahon, 2008; Murray et al., 1999; Shintou et al., 2007; Tarafdar et al., 2015). Interestingly, in the post-fusion *cis*-SNARE complex, the juxtamembrane motif associates with the t-SNAREs (Stein et al., 2009), suggesting that the juxtamembrane motif is dislodged from the membrane during a late stage of the fusion reaction. It is conceivable that dislodging of the juxtamembrane motif further disrupts the membrane structure at the fusion sites. Before its ultimate pairing with the t-SNAREs, the dislodged juxtamembrane motif may also transiently bind and destabilize the target membrane *in trans*. Together, these membrane-remodeling activities facilitate lipid rearrangements to form stalk and hemifusion intermediates, followed by opening and expansion of fusion pores controlled by SNARE transmembrane domains (Bao et al., 2016; Chang et al., 2015; Dhara et al., 2016; Fang and Lindau, 2014; Lindau et al., 2012; Ngatchou et al., 2010; Pieren et al., 2015).

The juxtamembrane motif of the v-SNARE is dispensable for the basal SNARE-driven membrane fusion, again demonstrating that the basal fusion reaction differs fundamentally from SNARE-SM-mediated membrane fusion (Yu et al., 2015, 2018). Only the SNARE-SM-mediated fusion recapitulates the intracellular vesicle fusion reaction. We posit that, without activation by a cognate SM protein, SNARE zippering proceeds through a different route that is not properly coupled to the activity of the juxtamembrane motif. Consistent with this model, the basal SNARE-driven fusion is insensitive to linker insertions, in stark contrast to the SNARE-SM-mediated fusion reaction. In a reconstituted fusion assay containing the Vc peptide, mutations of the juxtamembrane motif of VAMP2 decreased fusion kinetics (Hernandez et al., 2012). This observation can be explained by the discovery that the Vc peptide-assisted fusion reaction mimics SNARE-SM-mediated membrane fusion rather than the basal fusion reaction (Yu et al., 2018). Although the juxtamembrane motif of VAMP2 can associate with t-SNARE and Munc18-1 (Stein et al., 2009; Xu et al., 2010), our and others' data showed that the juxtamembrane motif is dispensable for SNARE-SNARE and SNARE-Munc18-1 interactions (Figure 3; Jiao et al., 2018).

The juxtamembrane region of the t-SNARE subunit syntaxin also positively regulates exocytosis (Lam et al., 2008; Singer-Lahat et al., 2018; van den Bogaart et al., 2011; Van Komen et al., 2005). However, this region lacks a hydrophobic stretch and is not known to penetrate into the surface of membrane bilayers (Lam et al., 2008). Thus, the juxtamembrane region of syntaxin may not act as a membrane-destabilizing peptide in the fusion reaction. Instead, the lipid-binding activity of this region may regulate syntaxin localization and/or modulate other exocytic factors. As discussed above, the juxtamembrane motif of the v-SNARE may bind and destabilize the target membrane *in trans* after its dislodging from the vesicle membrane, promoting lipid rearrangements in both membrane bilayers.

In this work, we focused on the conserved vesicle fusion machinery of SNAREs and SM proteins. In regulated exocytosis, the juxtamembrane motif of the v-SNARE is expected to act in concert with other membrane-remodeling molecules, such as synaptotagmin and Doc2b, to accelerate the fusion kinetics (Hui et al., 2009; Lynch et al., 2008; Martens et al., 2007; Martens and McMahon, 2008). Overall, our biochemical data agree well with genetic observations (Borisovska et al., 2012; Deák et al., 2006; DeMill et al., 2014; Kesavan et al., 2007; Williams et al., 2009). However, it should be noted that the juxtamembrane motif of VAMP2 also modulates the activities of specialized exocytic regulators such as Munc13 and complexin (Fang et al., 2013; Maximov et al., 2009; Wang et al., 2019). Because these binding modes can play opposite roles in exocytosis, mutations of specific residues in the juxtamembrane motif may lead to variable consequences *in vivo*, depending on cellular contexts and the nature of the mutations (Borisovska et al., 2012; Maximov et al., 2009; Williams et al., 2009).

STAR★METHODS

LEAD CONTACT AND MATERIALS AVAILABILITY

Further information and requests for resources and reagents should be directed to and will be fulfilled by the Lead Contact, Jingshi Shen (jingshi.shen@colorado.edu). All the reagents generated in this study are available via material transfer agreement.

EXPERIMENTAL MODEL AND SUBJECT DETAILS

Microbial Strains—All the recombinant proteins in this study were expressed in *E. Coli* BL21 [B F^- *ompT* hsdS(r_B^- m_B^-) dcm^+ Tet^r *gal* λ(DE3) *endA* Hte] at 37°C in a shaker incubator set at 220 rpm.

METHOD DETAILS

Recombinant protein expression and purification—Recombinant v- and t-SNARE proteins were expressed and purified as previously described (Shen et al., 2010). The t-SNARE complex was composed of untagged rat syntaxin-1 (full-length or cytoplasmic domain) and mouse SNAP-25 with an N-terminal His_6 tag cloned in the pTW34 expression vector. The v-SNARE protein (pET-SUMO-VAMP2) had no extra residue left after the His_6-SUMO tag was removed. Recombinant untagged Munc18-1 (from pET-SUMO-Munc18-1) and GST-tagged Munc18-1 proteins (from pGEX4T-3-Munc18-)) were produced in *E. coli* as previously described (Shen et al., 2007). The N-peptide (residues 1-35 of syntaxin-1) and

Vc peptide (residues 56-84 of VAMP2) were expressed and purified in *E. coli* using the pET28a vector (Rathore et al., 2010; Yu et al.,2018). SNARE mutants were prepared similarly as the corresponding WT proteins. Full-length SNAREs were stored in a buffer containing 25 mM HEPES (pH 7.4), 400 mM KCl, 1% n-octyl-β-D-glucoside (OG), 10% glycerol, and 0.5 mM Tris(2-carboxyethyl)phosphine (TCEP). Soluble proteins were stored in a protein binding buffer (25 mM HEPES [pH 7.4], 150 mM KCl, 10% glycerol, and 0.5 mM TCEP).

Proteoliposome reconstitution—To reconstitute t-SNARE liposomes for lipid-mixing assays, 1-palmitoyl-2-oleoyl-sn-glycero-3-phosphocholine (POPC), 1-palmitoyl-2-oleoyl-sn-glycero-3-phosphoethanolamine (POPE), 1-palmitoyl-2-oleoyl-sn-glycero-3-phosphoserine (POPS) and cholesterol were mixed in a molar ratio of 60:20:10:10. To prepare v-SNARE liposomes for lipid-mixing assays, POPC, POPE, POPS, cholesterol, (N-(7-nitro-2,1,3-benzoxadiazole-4-yl)-1,2-dipalmitoyl phosphatidylethanolamine (NBD-DPPE) and N-(Lissamine rhodamine B sulfonyl)-1,2-dipalmitoyl phosphatidylethanolamine (rhodamine-DPPE) were mixed at a molar ratio of 60:17:10:10:1.5:1.5. SNARE proteoliposomes were prepared by detergent dilution and isolated by Nycodenz density gradient flotation (Shen et al., 2010; Yu et al.,2018). Detergent was removed by overnight dialysis using Novagen dialysis tubes against the reconstitution buffer (25 mM HEPES [pH 7.4], 100 mM KCl, 10% glycerol, and 1 mM DTT). To prepare sulforhodamine B-loaded liposomes for content-mixing assays, v- and t-SNAREs were reconstituted in the presence of 50 mM sulforhodamine B. Free sulforhodamine B was removed by overnight dialysis followed by liposome flotation on a Nycodenz gradient. The protein: lipid ratio of v-SNARE liposomes was 1:200, similar to VAMP2 densities on native synaptic vesicles (Takamori et al., 2006), while the protein: lipid ratio of t-SNARE liposomes was 1:500. SNARE mutants were reconstituted into liposomes at the same molar densities as their respective WT proteins. Protein-free liposomes were prepared in a similar way as SNARE liposomes except that proteins were omitted.

Liposome fusion assays—Liposome fusion and data analysis were performed as previously described (Shen et al., 2010,2015; Yu et al., 2019). A standard liposome fusion reaction contained 5 mM t-SNAREs and 1.5 mM v-SNARE. In lipid-mixing assays, v-SNARE liposomes were labeled with NBD and rhodamine, and were directed to fuse with unlabeled t-SNARE liposomes with or without 5 mM Munc18-1 (Yu et al., 2019). The samples were incubated on ice for one hour before the temperature was elevated to 37°C to initiate fusion. NBD fluorescence (excitation: 460 nm; emission: 538 nm) was measured every two minutes in a BioTek Synergy HT microplate reader. In content-mixing assays, unlabeled t-SNARE liposomes were directed to fuse with sulforhodamine B-loaded v-SNARE liposomes. Sulforhodamine B fluorescence (excitation: 565; emission: 585 nm) was measured every two minutes. At the end of the reactions, 10 μL of 10% CHAPSO was added to each sample to lyse the liposomes to obtain the maximum fluorescence. Liposome fusion data were presented as the percentage of maximum fluorescence change. The maximum fusion rate within the first 10 minutes of a liposome fusion reaction was used to represent the initial rate. Statistical significance was calculated for each figure based on at least three experiments.

Liposome leakage assays—Sulforhodamine B-loaded protein-free liposomes were mixed with buffer or a SNARE peptide (added to a final concentration of 100 μM). Sulforhodamine B fluorescence was measured over time at 37°C. At the end of the reactions, 10 μL of 10% CHAPSO was added to lyse the liposomes to obtain the maximum fluorescence. The data are shown as percentage of maximum fluorescence. The N-peptide and Vc peptide were expressed and purified from *E. coli* whereas the juxtamembrane motif peptide of VAMP2 was synthesized by Biometik (95% purity). The sequences of the SNARE peptides are listed below:

N-peptide (residues 1-35 of syntaxin-1): MKDRTQELRTAKDSDDDDVTVTVDRDRFMDEFFE.

Vc peptide (residues 56-84 of VAMP2): RDQKLSELDDRADALQAGASQFETSAAKL.

Juxtamembrane motif peptide (residues 79-94 of VAMP2): TSAAKLKRKYWWKNLK.

Liposome co-flotation assay—Liposome co-flotation assay was carried out using a previously established procedure (Shen et al., 2007; Yu et al., 2018). Soluble proteins were incubated with protein-free or v-SNARE liposomes at 4°C with gentle agitation. After one hour, an equal volume of 80% (w/v) Nycodenz was added and the samples were transferred to 5 × 41 mm centrifuge tubes. The samples were overlaid with 200 μL each of 35% (w/v) and 30% (w/v) Nycodenz, and then with 20 μL reconstitution buffer on the top. All Nycodenz solutions were prepared in the reconstitution buffer. After centrifugation at 52,000 rpm for four hours in a Beckman SW55 rotor, samples were collected from the 0/30% Nycodenz interface and analyzed by SDS-PAGE.

ITC measurements—ITC experiments were performed at 25°C using a VP-ITC instrument (MicroCal). Munc18-1 and SNAREs were dialyzed overnight separately in an ITC binding buffer (25 mM HEPES [pH 7.4], 150 mM KCl, 10% Glycerol, and 0.5 mM TCEP) (Shen et al., 2015; Yu et al., 2013b). Munc18-1 protein (5 μM) was loaded into the sample cell of VP-ITC, followed by iterative injection of SNARE complexes (75 μM) into the sample cell. After polynomial baseline correction to remove a slight drift of the initial data points, the data were fitted with a nonlinear least-squares routine using the MicroCal Origin software.

Negative staining electron microscopy—Electron microscopy imaging of liposomes was carried out at Boulder Lab for 3D Electron Microscopy. Protein-free liposomes were incubated with buffer or a SNARE-derived peptide (added to a final concentration of 356 μM) for one hour at room temperature. The samples were then stained with 2% uranyl acetate and observed on a Philips CM100 scanning transmission electron microscope operated at 80 kV.

GST pull-down assay—Full-length ternary SNARE complexes were assembled as previously described (Shen et al., 2007). GST-Munc18-1 was expressed in *E. coli* using the pGEX4T-3-Munc18-1 plasmid and cell lysates were prepared using a protein binding buffer (25 mM HEPES [pH 7.4], 150 mM KCl, 10% glycerol, 1% CHAPS, and 1 mM DTT).

SNARE complexes were added to GST-Munc18-1-expressing *E. coli* ly-sates. After incubation at 4°C for one hour, glutathione Sepharose beads were added to the lysates to bind GST-Munc18-1 and associated proteins. After washing three times with the protein-binding buffer, protein complexes bound to the beads were resolved on SDS-PAGE and detected by immunoblotting using primary antibodies and horseradish peroxidase-conjugated secondary antibodies. The antibodies used in this work were polyclonal anti-Munc18-1 antibodies, monoclonal anti-syntaxin-1 antibodies, monoclonal anti-SNAP-25 antibodies, and monoclonal anti-VAMP2 antibodies.

QUANTIFICATION AND STATISTICAL ANALYSIS

Statistical significance was calculated for each data point based on at least three experiments. Data were analyzed using the KaleidaGraph 3.6 software (Synergy) and are presented as means ± standard deviation.

DATA AND CODE AVAILABILITY

This study did not generate code or dataset.

Supplementary Material

Refer to Web version on PubMed Central for supplementary material.

ACKNOWLEDGMENTS

We thank Drs. Josep Rizo, Manfred Lindau, Yongli Zhang, Wolfhard Almers, Stephen Harrison, Michael Kozlov, Tijana Ivanovic, and Richard Epand for reagents or discussions and Yan Ouyang for technical assistance. This work was supported by NIH grants GM126960 (to J.S.), DK095367 (to J.S.), AG061829 (to J.S. and M.H.B.S.), and AI135473 (to H.Y.); an American Diabetes Association basic science award (to J.S.); and a University of Colorado seed grant (to J.S.). Publication of this article was partially funded by the University of Colorado Boulder Libraries Open Access Fund.

REFERENCES

Allison SL, Stiasny K, Stadler K, Mandl CW, and Heinz FX (1999). Mapping of functional elements in the stem-anchor region of tick-borne encephalitis virus envelope protein E. J. Virol 73, 5605–5612. [PubMed: 10364309]

Bailey AL, Monck MA, and Cullis PR (1997). pH-induced destabilization of lipid bilayers by a lipopeptide derived from influenza hemagglutinin. Biochim. Biophys. Acta 1324, 232–244.

Baker RW, and Hughson FM (2016). Chaperoning SNARE assembly and disassembly. Nat. Rev. Mol. Cell Biol 17, 465–79. [PubMed: 27301672]

Baker RW, Jeffrey PD, Zick M, Phillips BP, Wickner WT, and Hughson FM (2015). A direct role for the Sec1/Munc18-family protein Vps33 as a template for SNARE assembly. Science 349, 1111–1114. [PubMed: 26339030]

Bao H, Goldschen-Ohm M, Jeggle P, Chanda B, Edwardson JM, and Chapman ER (2016). Exocytotic fusion pores are composed of both lipids and proteins. Nat. Struct. Mol. Biol 23, 67–73. [PubMed: 26656855]

Borisovska M, Schwarz YN, Dhara M, Yarzagaray A, Hugo S, Narzi D, Siu SW, Kesavan J, Mohrmann R, Bockmann RA, and Bruns D (2012). Membrane-proximal tryptophans of synaptobrevin II stabilize priming of secretory vesicles. J. Neurosci 32, 15983–15997. [PubMed: 23136435]

Bowen M, and Brunger AT (2006). Conformation of the synaptobrevin transmembrane domain. Proc. Natl. Acad. Sci. USA 103, 8378–8383. [PubMed: 16709671]

Brewer KD, Li W, Horne BE, and Rizo J (2011). Reluctanceto membrane binding enables accessibility of the synaptobrevin SNARE motif for SNARE complex formation. Proc. Natl. Acad. Sci. USA 108, 12723–12728. [PubMed: 21768342]

Brunger AT, Weninger K, Bowen M, and Chu S (2009). Single-molecule studies of the neuronal SNARE fusion machinery. Annu. Rev. Biochem 78, 903–928. [PubMed: 19489736]

Buzon V, Natrajan G, Schibli D, Campelo F, Kozlov MM, and Weissenhorn W (2010). Crystal structure of HIV-1 gp41 including both fusion peptide and membrane proximal external regions. PLoS Pathog. 6, e1000880. [PubMed: 20463810]

Chang CW, Hui E, Bai J, Bruns D, Chapman ER, and Jackson MB (2015). A structural role for the synaptobrevin 2 transmembrane domain in densecore vesicle fusion pores. J. Neurosci 35, 5772–5780. [PubMed: 25855187]

Chernomordik LV, and Kozlov MM (2003). Protein-lipid interplay in fusion and fission of biological membranes. Annu. Rev. Biochem 72, 175–207. [PubMed: 14527322]

Chernomordik LV, and Kozlov MM (2008). Mechanics of membrane fusion. Nat. Struct. Mol. Biol 15, 675–683. [PubMed: 18596814]

Chlanda P, Mekhedov E, Waters H, Schwartz CL, Fischer ER, Ryham RJ, Cohen FS, Blank PS, and Zimmerberg J (2016). The hemifusion structure induced by influenzavirus haemagglutinin is determined by physical properties of the target membranes. Nat. Microbiol 1, 16050. [PubMed: 27572837]

Deák F, Shin OH, Kavalali ET, and Südhof TC (2006). Structural determinants of synaptobrevin 2 function in synaptic vesicle fusion. J. Neurosci 26, 6668–6676. [PubMed: 16793874]

DeMill CM, Qiu X, Kisiel M, Bolotta A, and Stewart BA (2014). Investigation of the juxtamembrane region of neuronal-Synaptobrevin in synaptic transmission at the Drosophila neuromuscular junction. J. Neurophysiol 112, 1356–1366. [PubMed: 24944220]

Dhara M, Yarzagaray A, Makke M, Schindeldecker B, Schwarz Y, Shaaban A, Sharma S, Bockmann RA, Lindau M, Mohrmann R, and Bruns D (2016). v-SNARE transmembrane domains function as catalysts for vesicle fusion. eLife 5, e17571. [PubMed: 27343350]

Domanska MK, Kiessling V, Stein A, Fasshauer D, and Tamm LK (2009). Single vesicle millisecond fusion kinetics reveals number of SNARE complexes optimal for fast SNARE-mediated membrane fusion. J. Biol. Chem 284, 32158–32166. [PubMed: 19759010]

Düzgüneş N, and Shavnin SA (1992). Membrane destabilization by N-terminal peptides of viral envelope proteins. J. Membr. Biol 128, 71–80. [PubMed: 1323686]

Earp LJ, Delos SE, Park HE, and White JM (2005). The many mechanisms of viral membrane fusion proteins. Curr. Top. Microbiol. Immunol 285, 25–66. [PubMed: 15609500]

Ellena JF, Liang B, Wiktor M, Stein A, Cafiso DS, Jahn R, and Tamm LK (2009). Dynamic structure of lipid-bound synaptobrevin suggests a nucleation-propagation mechanism for trans-SNARE complex formation. Proc. Natl. Acad. Sci. USA 106, 20306–20311. [PubMed: 19918058]

Epand RM (2003). Fusion peptides and the mechanism of viral fusion. Biochim. Biophys. Acta 1614, 116–121. [PubMed: 12873772]

Fang Q, and Lindau M (2014). How could SNARE proteins open a fusion pore? Physiology (Bethesda) 29, 278–285. [PubMed: 24985331]

Fang Q, Zhao Y, and Lindau M (2013). Juxtamembrane tryptophans of synaptobrevin 2 control the process of membrane fusion. FEBS Lett. 587, 67–72. [PubMed: 23178715]

Faust JE, Desai T, Verma A, Ulengin I, Sun TL, Moss TJ, Betancourt-Solis MA, Huang HW, Lee T, and McNew JA (2015). The Atlastin C-terminal tail is an amphipathic helix that perturbs the bilayer structure during endoplasmic reticulum homotypic fusion. J. Biol. Chem 290, 4772–4783. [PubMed: 25555915]

Haldar S, Mekhedov E, McCormick CD, Blank PS, and Zimmerberg J (2018). Lipid-dependence of target membrane stability during influenza viral fusion. J. Cell Sci 132, jcs218321. [PubMed: 29967032]

Han J, Pluhackova K, Bruns D, and Bockmann RA (2016). Synaptobrevin transmembrane domain determines the structure and dynamics of the SNARE motif and the linker region. Biochim. Biophys. Acta 1858, 855–865. [PubMed: 26851777]

Harrison SC (2008). Viral membrane fusion. Nat. Struct. Mol. Biol 15, 690–698. [PubMed: 18596815]

Hernandez JM, Stein A, Behrmann E, Riedel D, Cypionka A, Farsi Z, Walla PJ, Raunser S, and Jahn R (2012). Membrane fusion intermediates via directional and full assembly of the SNARE complex. Science 336, 1581–1584. [PubMed: 22653732]

Howard MW, Travanty EA, Jeffers SA, Smith MK, Wennier ST, Thackray LB, and Holmes KV (2008). Aromatic amino acids in the juxtamembrane domain of severe acute respiratory syndrome coronavirus spike glycoprotein are important for receptor-dependent virus entry and cell-cell fusion. J. Virol 82, 2883–2894. [PubMed: 18199653]

Hu SH, Christie MP, Saez NJ, Latham CF, Jarrott R, Lua LH, Collins BM, and Martin JL (2011). Possible roles for Munc18-1 domain 3a and Syntaxin1 N-peptide and C-terminal anchor in SNARE complex formation. Proc. Natl. Acad. Sci. USA 108, 1040–1045. [PubMed: 21193638]

Huang Q, Chen CL, and Herrmann A (2004). Bilayer conformation of fusion peptide of influenza virus hemagglutinin: a molecular dynamics simulation study. Biophys. J 87, 14–22. [PubMed: 15240440]

Hui E, Johnson CP, Yao J, Dunning FM, and Chapman ER (2009). Synaptotagmin-mediated bending of the target membrane is a critical step in Ca(2+)-regulated fusion. Cell 138, 709–721. [PubMed: 19703397]

Jeetendra E, Ghosh K, Odell D, Li J, Ghosh HP, and Whitt MA (2003). The membrane-proximal region of vesicular stomatitis virus glycoprotein G ectodomain is critical for fusion and virus infectivity. J. Virol 77, 12807–12818. [PubMed: 14610202]

Jiao J, He M, Port SA, Baker RW, Xu Y, Qu H, Xiong Y, Wang Y, Jin H, Eisemann TJ, et al. (2018). Munc18-1 catalyzes neuronal SNARE assembly by templating SNARE association. eLife 7, e41771. [PubMed: 30540253]

Kesavan J, Borisovska M, and Bruns D (2007). v-SNARE actions during Ca(2+)-triggered exocytosis. Cell 131, 351–363. [PubMed: 17956735]

Kozlov MM, McMahon HT, and Chernomordik LV (2010). Protein-driven membrane stresses in fusion and fission. Trends Biochem. Sci 35, 699–706. [PubMed: 20638285]

Krämer L, and Ungermann C (2011). HOPS drives vacuole fusion by binding the vacuolar SNARE complex and the Vam7 PX domain via two distinct sites. Mol. Biol. Cell 22, 2601–2611. [PubMed: 21613544]

Kweon DH, Kim CS, and Shin YK (2003). Regulation of neuronal SNARE assembly by the membrane. Nat. Struct. Biol 10, 440–447. [PubMed: 12740606]

Lam AD, Tryoen-Toth P, Tsai B, Vitale N, and Stuenkel EL (2008). SNARE-catalyzed fusion events are regulated by Syntaxin1A-lipid interactions. Mol. Biol. Cell 19, 485–497. [PubMed: 18003982]

Lamb RA, and Jardetzky TS (2007). Structural basis of viral invasion: lessons from paramyxovirus F. Curr. Opin. Struct. Biol 17, 427–436. [PubMed: 17870467]

Lindau M, Hall BA, Chetwynd A, Beckstein O, and Sansom MSP (2012). Coarse-grain simulations reveal movement of the synaptobrevin C-terminus in response to piconewton forces. Biophys. J 103, 959–969. [PubMed: 23009845]

Liu TY, Bian X, Sun S, Hu X, Klemm RW, Prinz WA, Rapoport TA, and Hu J (2012). Lipid interaction of the C terminus and association of the transmembrane segments facilitate atlastin-mediated homotypic endoplasmic reticulum fusion. Proc. Natl. Acad. Sci. USA 109, E2146–E2154. [PubMed: 22802620]

Lynch KL, Gerona RR, Kielar DM, Martens S, McMahon HT, and Martin TF (2008). Synaptotagmin-1 utilizes membrane bending and SNARE binding to drive fusion pore expansion. Mol. Biol. Cell 19, 5093–5103. [PubMed: 18799625]

Ma C, Su L, Seven AB, Xu Y, and Rizo J (2013). Reconstitution of the vital functions of Munc18 and Munc13 in neurotransmitter release. Science 339,421–25. [PubMed: 23258414]

Martens S, and McMahon HT (2008). Mechanisms of membrane fusion: disparate players and common principles. Nat. Rev. Mol. Cell Biol 9, 543–556. [PubMed: 18496517]

Martens S, Kozlov MM, and McMahon HT (2007). How synaptotagmin promotes membrane fusion. Science316, 1205–1208. [PubMed: 17478680]

Martin S, Tomatis VM, Papadopulos A, Christie MP, Malintan NT, Gormal RS, Sugita S, Martin JL, Collins BM, and Meunier FA (2013). The Munc18-1 domain 3a loop is essential for

neuroexocytosis but not for syntaxin-1A transport to the plasma membrane. J. Cell Sci 126, 2353–2360. [PubMed: 23761923]

Maximov A, Tang J, Yang X, Pang ZP, and Südhof TC (2009). Complexin controls the force transfer from SNARE complexes to membranes in fusion. Science 323, 516–521. [PubMed: 19164751]

McMahon HT, Kozlov MM, and Martens S (2010). Membrane curvature in synaptic vesicle fusion and beyond. Cell 140, 601–605. [PubMed: 20211126]

Mohrmann R, de Wit H, Verhage M, Neher E, and Sørensen JB (2010). Fast vesicle fusion in living cells requires at least three SNARE complexes. Science 330, 502–505. [PubMed: 20847232]

Montal M (1999). Electrostatic attraction at the core of membrane fusion. FEBS Lett. 447, 129–130. [PubMed: 10214931]

Munoz-Barroso I, Salzwedel K, Hunter E, and Blumenthal R (1999). Role of the membrane-proximal domain in the initial stages of human immunodeficiency virus type 1 envelope glycoprotein-mediated membrane fusion. J. Virol 73, 6089–6092. [PubMed: 10364363]

Murray D, Arbuzova A, Hangyás-Mihályné G, Gambhir A, Ben-Tal N, Honig B, and McLaughlin S (1999). Electrostatic properties of membranes containing acidic lipids and adsorbed basic peptides: theory and experiment. Biophys. J 77, 3176–3188. [PubMed: 10585939]

Ngatchou AN, Kisler K, Fang Q, Walter AM, Zhao Y, Bruns D, Sorensen JB, and Lindau M(2010). Role of the synaptobrevin C terminus in fusion pore formation. Proc. Natl. Acad. Sci. USA 107, 18463–18468. [PubMed: 20937897]

Ohya T, Miaczynska M, Coskun U, Lommer B, Runge A, Drechsel D, Kalaidzidis Y, and Zerial M (2009). Reconstitution of Rab- and SNARE-dependent membrane fusion by synthetic endosomes. Nature 459, 1091–1097. [PubMed: 19458617]

Pieren M, Desfougères Y, Michaillat L, Schmidt A, and Mayer A (2015). Vacuolar SNARE protein transmembrane domains serve as nonspecific membrane anchors with unequal roles in lipid mixing. J. Biol. Chem 290, 12821–12832. [PubMed: 25817997]

Rathore SS, Bend EG, Yu H, Hammarlund M, Jorgensen EM, and Shen J (2010). Syntaxin N-terminal peptide motif is an initiation factor for the assembly of the SNARE-Sec1/Munc18 membrane fusion complex. Proc. Natl. Acad. Sci. USA 107, 22399–22406. [PubMed: 21139055]

Risselada HJ, and Grubmüller H (2012). How SNARE molecules mediate membrane fusion: recent insights from molecular simulations. Curr. Opin. Struct. Biol 22, 187–196. [PubMed: 22365575]

Rizo J, and Südhof TC (2012). The membrane fusion enigma: SNAREs, Sec1/Munc18 proteins, and their accomplices–guilty as charged? Annu. Rev. Cell Dev. Biol 28, 279–308. [PubMed: 23057743]

Schwartz ML, and Merz AJ (2009). Capture and release of partially zipped trans-SNARE complexes on intact organelles. J. Cell Biol 185, 535–549. [PubMed: 19414611]

Shen J, Tareste DC, Paumet F, Rothman JE, and Melia TJ (2007). Selective activation of cognate SNAREpins by Sec1/Munc18 proteins. Cell 128, 183–195. [PubMed: 17218264]

Shen J, Rathore SS, Khandan L, and Rothman JE (2010). SNARE bundle and syntaxin N-peptide constitute a minimal complement for Munc18-1 activation of membrane fusion. J. Cell Biol 190, 55–63. [PubMed: 20603329]

Shen C, Rathore SS, Yu H, Gulbranson DR, Hua R, Zhang C, Schoppa NE, and Shen J (2015). The trans-SNARE-regulating function of Munc18-1 is essential to synaptic exocytosis. Nat. Commun 6, 8852. [PubMed: 26572858]

Shi L, Shen QT, Kiel A, Wang J, Wang HW, Melia TJ, Rothman JE, and Pincet F (2012). SNARE proteins: one to fuse and three to keep the nascent fusion pore open. Science 335, 1355–1359. [PubMed: 22422984]

Shintou K, Nakano M, Kamo T, Kuroda Y, and Handa T (2007). Interaction of an amphipathic peptide with phosphatidycholine/phosphatidylethanolamine mixed membranes. Biophys. J 93, 3900–3906. [PubMed: 17704174]

Shmulevitz M, Epand RF, Epand RM, and Duncan R (2004). Structural and functional properties of an unusual internal fusion peptide in a nonenveloped virus membrane fusion protein. J. Virol. 78, 2808–2818. [PubMed: 14990700]

Singer-Lahat D, Barak-Broner N, Sheinin A, Greitzer-Antes D, Michaelevski I, and Lotan I (2018). The Dual Function of the Polybasic Juxtamembrane Region of Syntaxin 1A in Clamping

Spontaneous Release and Stimulating Ca^{2+}-Triggered Release in Neuroendocrine Cells. J. Neurosci 38, 220–231. [PubMed: 29133430]

Söllner T, Whiteheart SW, Brunner M, Erdjument-Bromage H, Geromanos S, Tempst P, and Rothman JE (1993). SNAP receptors implicated in vesicle targeting and fusion. Nature 362, 318–324. [PubMed: 8455717]

Stein A, Weber G, Wahl MC, and Jahn R (2009). Helical extension of the neuronal SNARE complex into the membrane. Nature 460, 525–528. [PubMed: 19571812]

Südhof TC, and Rothman JE (2009). Membrane fusion: grappling with SNARE and SM proteins. Science 323, 474–477. [PubMed: 19164740]

Takamori S, Holt M, Stenius K, Lemke EA, Gronborg M, Riedel D, Urlaub H, Schenck S, Brügger B, Ringler P, et al. (2006). Molecular anatomy of a trafficking organelle. Cell 127, 831–846. [PubMed: 17110340]

Tarafdar PK, Chakraborty H, Bruno MJ, and Lentz BR (2015). Phosphatidylserine-Dependent Catalysis of Stalk and Pore Formation by Synaptobrevin JMR-TMD Peptide. Biophys. J 109, 1863–1872. [PubMed: 26536263]

Thorén PE, Persson D, Lincoln P, and Nordén B (2005). Membrane destabilizing properties of cell-penetrating peptides. Biophys. Chem 114, 169–179. [PubMed: 15829350]

Top D, deAntueno R, Salsman J, Corcoran J, Mader J, Hoskin D, Touhami A, Jericho MH, and Duncan R (2005). Liposome reconstitution of a minimal protein-mediated membrane fusion machine. EMBO J. 24, 2980–2988. [PubMed: 16079913]

van den Bogaart G, Meyenberg K, Risselada HJ, Amin H, Willig KI, Hubrich BE, Dier M, Hell SW, Grubmüller H, Diederichsen U, and Jahn R (2011). Membrane protein sequestering by ionic protein-lipid interactions. Nature 479, 552–555. [PubMed: 22020284]

Van Komen JS, Bai X, Rodkey TL, Schaub J, and McNew JA (2005). The polybasic juxtamembrane region of Sso1p is required for SNARE function in vivo. Eukaryot. Cell 4, 2017–2028. [PubMed: 16339720]

Vishwanathan SA, and Hunter E (2008). Importance of the membrane-perturbing properties of the membrane-proximal external region of human immunodeficiency virus type 1 gp41 to viral fusion. J. Virol 82, 5118–5126. [PubMed: 18353966]

Walter AM, Wiederhold K, Bruns D, Fasshauer D, and Sørensen JB (2010). Synaptobrevin N-terminally bound to syntaxin-SNAP-25 defines the primed vesicle state in regulated exocytosis. J. Cell Biol 188, 401–413. [PubMed: 20142423]

Wang S, Li Y, Gong J, Ye S, Yang X, Zhang R, and Ma C (2019). Munc18 and Munc13 serve as a functional template to orchestrate neuronal SNARE complex assembly. Nat. Commun 10, 69. [PubMed: 30622273]

Weber T, Parlati F, McNew JA, Johnston RJ, Westermann B, Sollner TH, and Rothman JE (1998). SNAREpins are functionally resistant to disruption by NSF and alphaSNAP. J. Cell Biol, 1063–1072.

Wickner W (2010). Membrane fusion: five lipids, four SNAREs, three chaperones, two nucleotides, and a Rab, all dancing in a ring on yeast vacuoles. Annu. Rev. Cell Dev. Biol 26, 115–136. [PubMed: 20521906]

Williams D, Vicôgne J, Zaitseva I, McLaughlin S, and Pessin JE (2009). Evidence that electrostatic interactions between vesicle-associated membrane protein 2 and acidic phospholipids may modulate the fusion of transport vesicles with the plasma membrane. Mol. Biol. Cell 20, 4910–4919. [PubMed: 19812247]

Xu Y, Su L, and Rizo J (2010). Binding of Munc18-1 to synaptobrevin and to the SNARE four-helix bundle. Biochemistry 49, 1568–1576. [PubMed: 20102228]

Yu H, Rathore SS, Lopez JA, Davis EM, James DE, Martin JL, and Shen J (2013a). Comparative studies of Munc18c and Munc18-1 reveal conserved and divergent mechanisms of Sec1/Munc18 proteins. Proc. Natl. Acad. Sci. USA 110, E3271–E3280. [PubMed: 23918365]

Yu H, Rathore SS, and Shen J (2013b). Synip arrests soluble N-ethylmaleimide-sensitive factor attachment protein receptor (SNARE)-dependent membrane fusion as a selective target membrane SNARE-binding inhibitor. J. Biol. Chem 288, 18885–18893. [PubMed: 23665562]

Yu H, Rathore SS, Shen C, Liu Y, Ouyang Y, Stowell MH, and Shen J (2015). Reconstituting Intracellular Vesicle Fusion Reactions: The Essential Role of Macromolecular Crowding. J. Am. Chem. Soc 137, 12873–12883. [PubMed: 26431309]

Yu H, Shen C, Liu Y, Menasche BL, Ouyang Y, Stowell MHB, and Shen J (2018). SNARE zippering requires activation by SNARE-like peptides in Sec1/Munc18 proteins. Proc. Natl. Acad. Sci. USA 115, E8421–E8429. [PubMed: 30127032]

Yu H, Crisman L, Stowell MHB, and Shen J (2019). Functional Reconstitution of Intracellular Vesicle Fusion Using Purified SNAREs and Sec1/Munc18 (SM) Proteins. Methods Mol. Biol 1860, 237–249. [PubMed: 30317509]

Highlights

- The juxtamembrane motif of the v-SNARE is essential for vesicle fusion
- The juxtamembrane motif directly destabilizes the lipid bilayer
- The function of the juxtamembrane motif requires both polar and nonpolar residues
- Linker insertions between SNARE and juxtamembrane motifs impair vesicle fusion

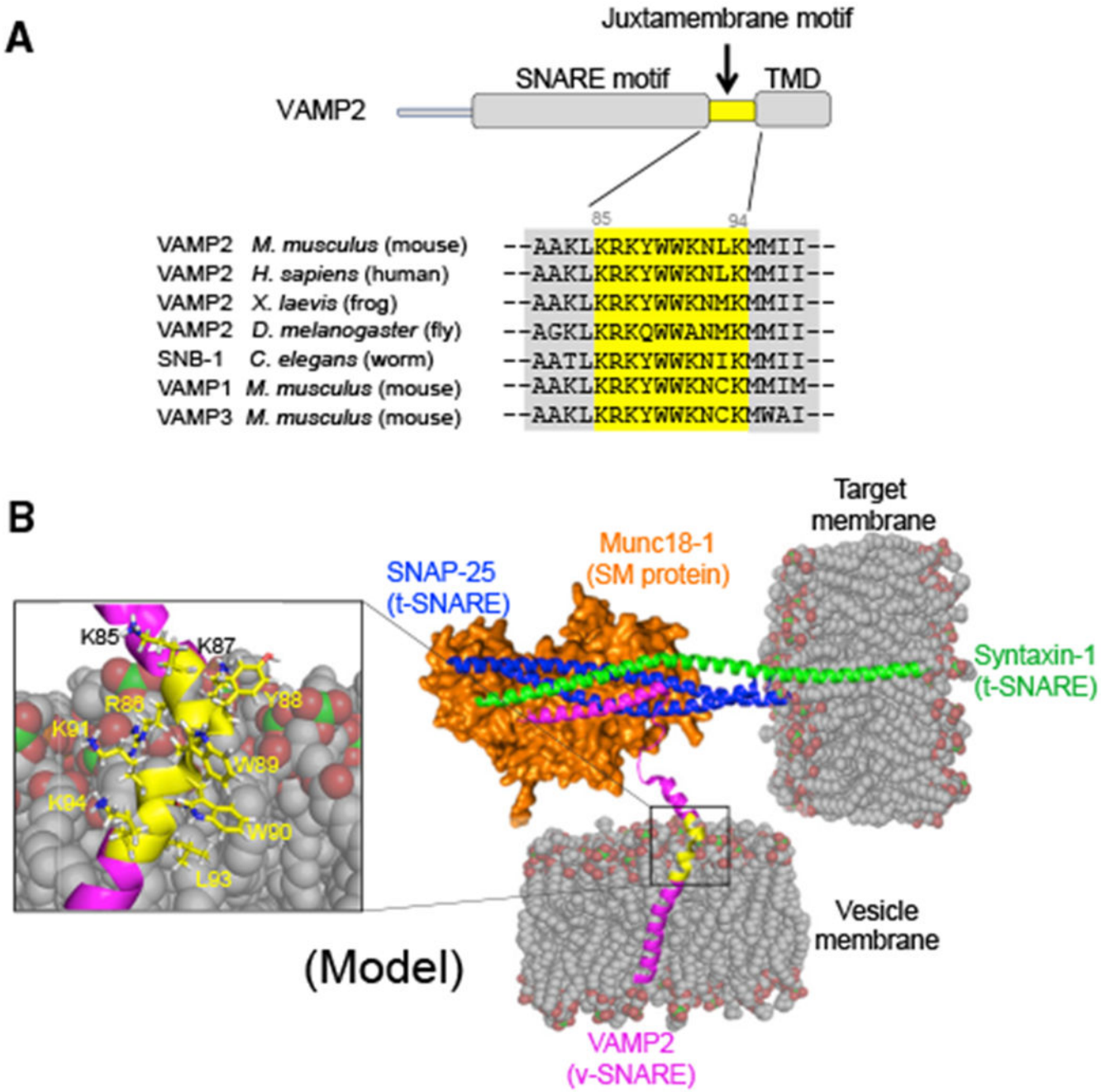

Figure 1. The Juxtamembrane Motif of the v-SNARE Is Embedded in the Surface of the Lipid Bilayer

(A) Sequence alignment of the juxtamembrane motifs (highlighted in yellow) of exocytic v-SNAREs from multiple species. The SNARE motif is also known as the core domain. TMD, transmembrane domain.

(B) Model of the VAMP2 juxtamembrane motif embedded in a membrane bilayer. Magenta, VAMP2 (v-SNARE, the juxtamembrane motif is highlighted in yellow); green, syntaxin-1 (t-SNARE); blue, SNAP-25 (t-SNARE, only the SNARE motifs are shown); orange, Munc18-1 (SM protein, shown as a surface model). The juxtamembrane motif of VAMP2 is

based on previous biophysical and structural data (Bowen and Brunger, 2006; Brewer et al., 2011; Ellena et al., 2009; Kweon et al., 2003). The TMD of VAMP2 is tilted about 35° relative to the membrane normal to allow the nonpolar residues of the juxtamembrane motif to insert into the hydrophobic phase of the bilayer and the basic residues to embed in the hydrophilic phase of the membrane. Carbon, oxygen, and phosphorus atoms of the lipid bilayer are colored gray, red, and green, respectively. The model is based on the structures of the v-SNARE (PDB: 2KOG; Ellena et al., 2009), the *cis*-SNARE complex (PDB: 3HD7; Stein et al., 2009), and Munc18-1 (PDB: 3PUJ; Hu et al., 2011). Because the structure of Munc18-1 bound to the half-zippered *trans*-SNARE complex has not been determined, the position of Munc18-1 depicted in the model is arbitrary. The model of the phosphatidylcholine bilayer (popc128a.pdb) was obtained from the Department of Biocomputing at the University of Calgary (Calgary, AB, Canada). The models were prepared using PyMOL (DeLano Scientific LLC, San Carlos, CA).

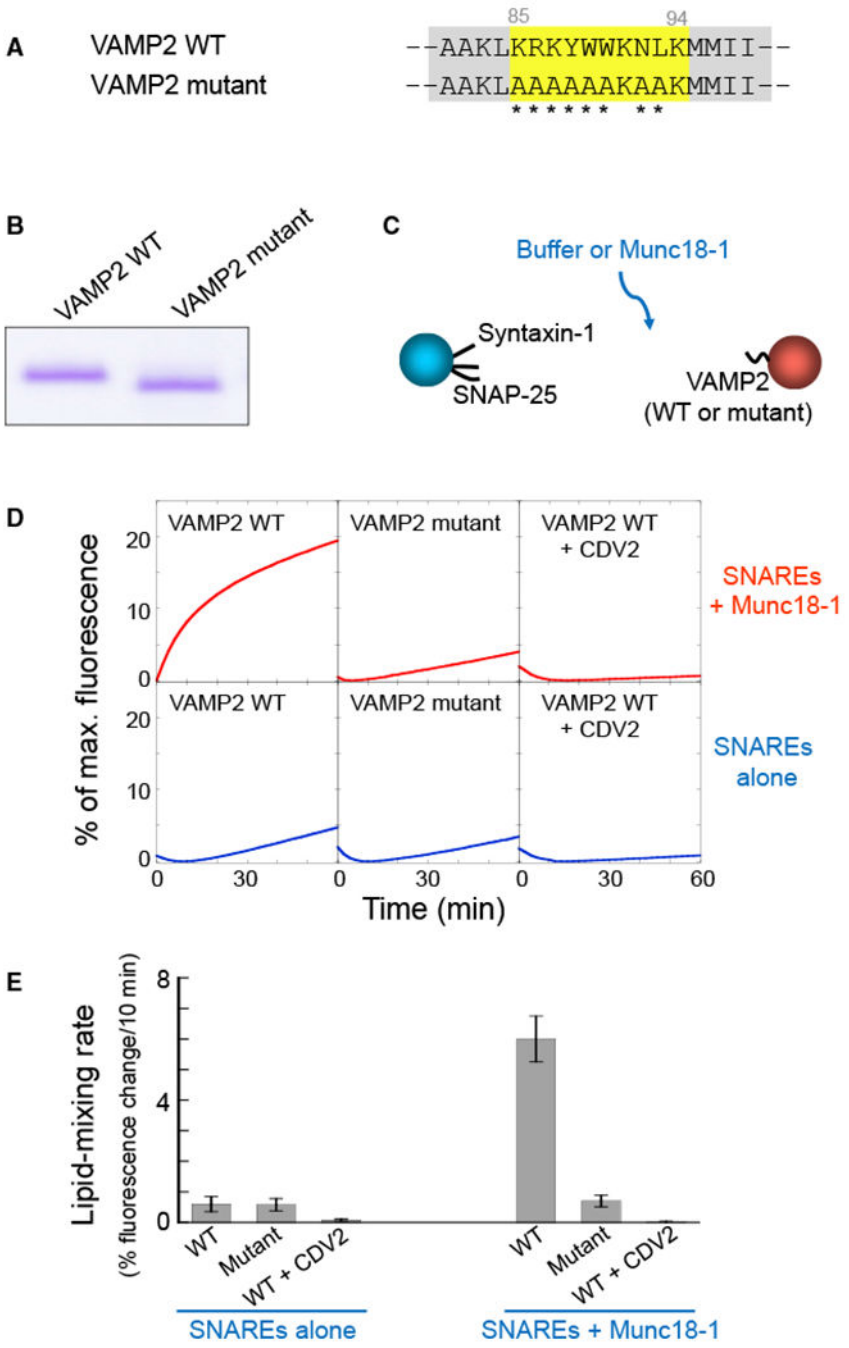

Figure 2. The Juxtamembrane Motif of VAMP2 Is Essential for SNARE-Munc18-1-Mediated Membrane Fusion

(A) Sequence alignment of the juxtamembrane motifs of WT VAMP2 and a VAMP2 mutant in which the juxtamembrane motif was mutated into alanines. Asterisks indicate the conserved residues mutated in the VAMP2 mutant. Lysine 94 (K94) was not mutated because this basic residue demarcates the boundary of the TMD. Lysine 91 (K91) was not mutated because it is not evolutionarily conserved. Nevertheless, identical results were observed when K91 was also mutated (Figure 6).

(B) Representative Coomassie blue-stained gel showing that WT and mutant VAMP2 proteins were reconstituted into proteoliposomes at comparable levels.
(C) Diagram of liposome pairs in the reconstituted liposome fusion reactions. WT t-SNARE liposomes were directed to fuse with v-SNARE liposomes containing WT or mutant VAMP2 in the absence or presence of 5 μM Munc18-1.
(D) Lipid mixing of the liposome fusion reactions. In negative control reactions, the dominant-negative inhibitor CDV2 (cytoplasmic domain of VAMP2) was added to a final concentration of 20 μM. Content mixing of the liposomes is shown in Figure S2.
(E) Initial lipid-mixing rates of the liposome fusion reactions in (D). Data are presented as average percentage of fluorescence change within the initial 10 min of the reactions based on three independent experiments. Error bars indicate SD.
See also Figures S1 and S2.

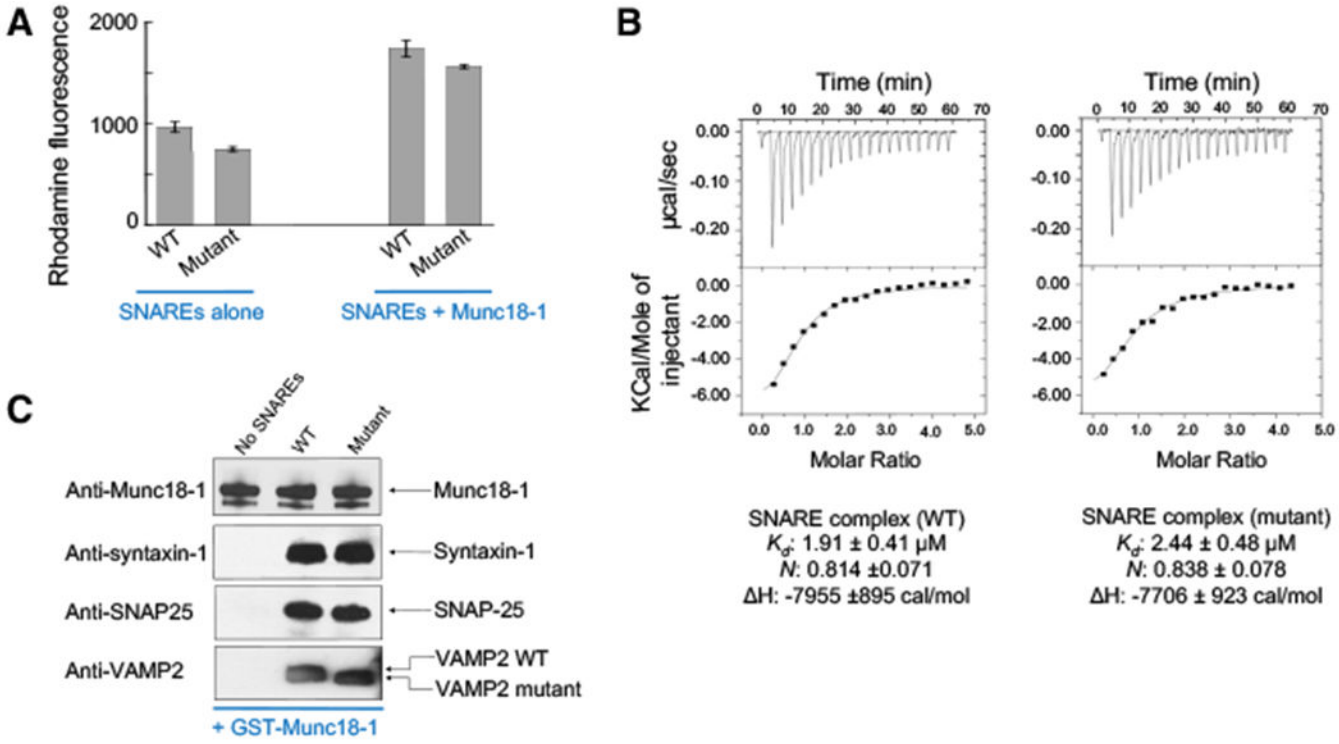

Figure 3. The Juxtamembrane Motif of VAMP2 Is Dispensable for SNARE-Munc18-1 Association

(A) Measurements of the docking of t- and v-SNARE liposomes using a liposome docking assay (Yu et al., 2013a). Biotin-labeled WT t-SNARE liposomes were anchored to avidin agarose beads and used to bind rhodamine-labeled v-SNARE liposomes (WT or mutant). The VAMP2 mutant is depicted in Figure 2A. The binding reactions were carried out at 4°C for 1 h in the absence or presence of 5 µM Munc18-1. Biotin-labeled protein-free liposomes were used as a negative control to obtain the background fluorescent signal, which was subtracted from other binding reactions to alculate SNARE-dependent liposome docking. The data are presented as average fluorescence intensity of rhodamine bound to the beads based on three independent experiments. Error bars indicate SD.

(B) Measurements of SNARE-Munc18-1 association using ITC. The ternary SNARE complexes were assembled from the cytoplasmic domains of v- and t-SNAREs: VAMP2 (residues 1–95, WT or mutant), syntaxin-1 (residues 1–265), and full-length SNAP-25 (Yu et al., 2013a). The dissociation constant of the SNARE-Munc18-1 complex was calculated by fitting the data with a nonlinear least-squares routine using the MicroCal Origin software.

(C) Representative immunoblots showing the binding of WT or mutant SNARE complexes to GST-Munc18-1. GST-Munc18-1 proteins bound to glutathione Sepharose beads were used to precipitate full-length ternary SNARE complexes using a previously established procedure (Shen et al., 2010). Protein complexes in the precipitates were resolved on SDS-PAGE and analyzed by immunoblotting using the indicated antibodies.

See also Figure S3.

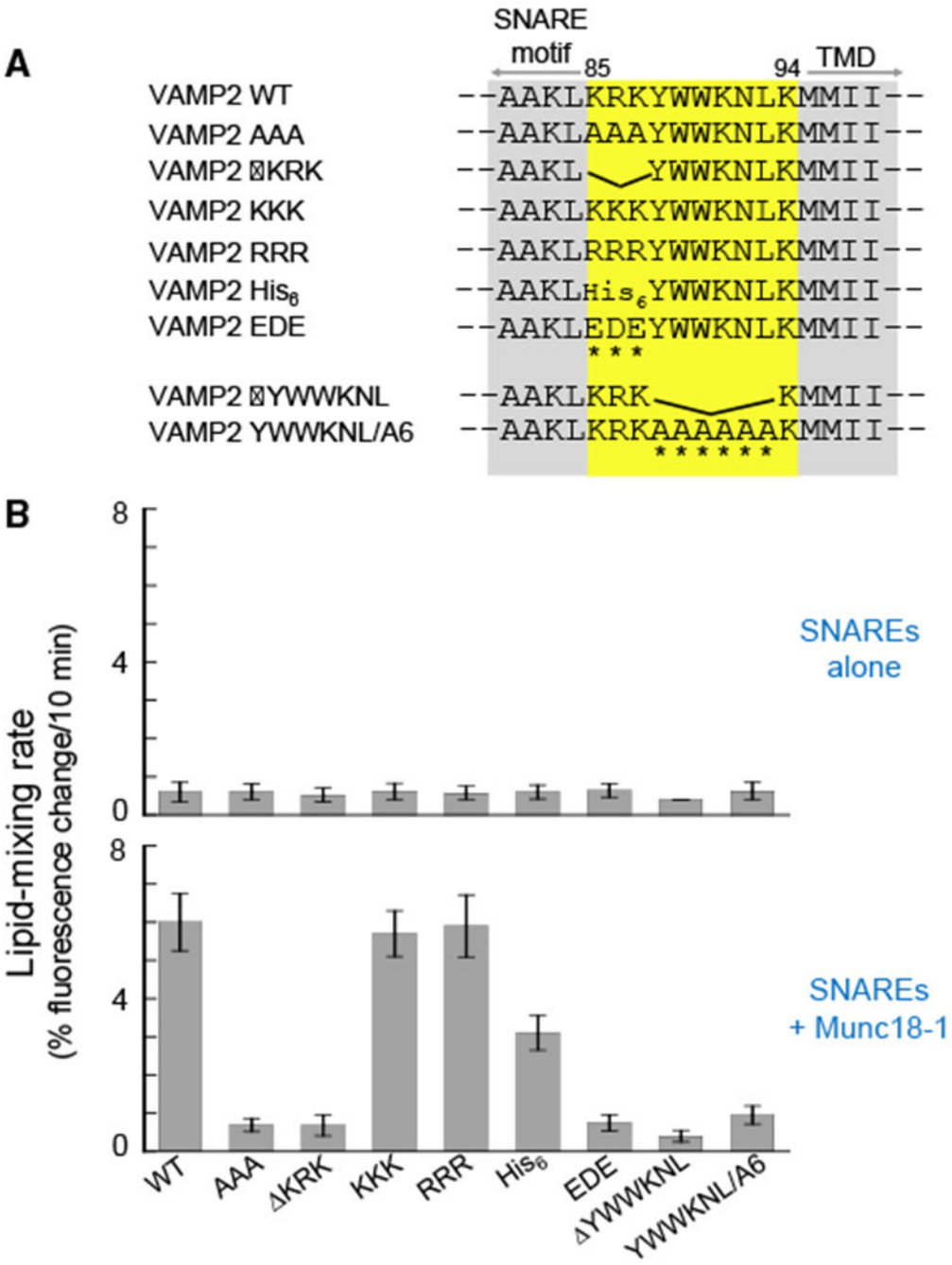

Figure 4. The Function of the VAMP2 Juxtamembrane Motif Requires Both Basic and Hydrophobic Residues

(A) Sequence alignment of juxtamembrane motifs (highlighted in yellow) in WT and mutant VAMP2. The mutated residues are indicated with asterisks.

(B) Initial lipid mixing rates of the liposome fusion reactions. WT t-SNARE liposomes were directed to fuse with WT or mutant v-SNARE liposomes in the presence or absence of 5 μM Munc18-1. Data are presented as the average percentage of fluorescence change within the initial 10 min of the reactions based on three independent experiments. Error bars indicate SD.

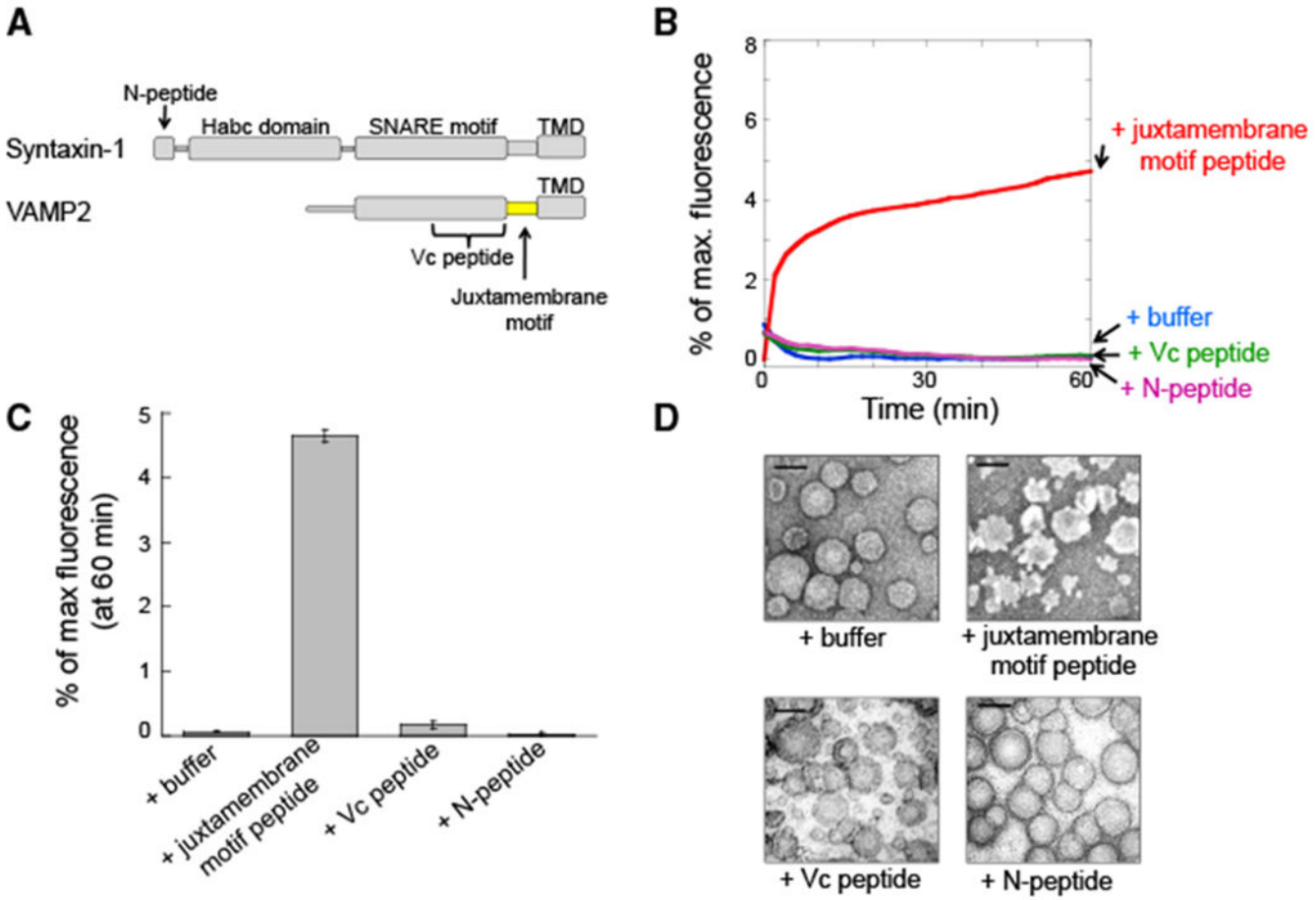

Figure 5. The Juxtamembrane Motif of VAMP2 Destabilizes the Membrane Bilayer

(A) Diagrams showing the SNARE-derived peptides: the N-peptide (residues 1–35) of syntaxin-1, the Vc peptide (residues 56–84) of VAMP2, and the juxtamembrane motif (residues 79–94) of VAMP2.

(B) Sulforhodamine B-loaded protein-free liposomes were incubated with buffer or the indicated peptides at 37°C for 60 min, and sulforhodamine B fluorescence during the incubation was measured. Liposome leakage leads to sulforhodamine B dequenching and increases in its fluorescence. Each peptide was added to a final concentration of 100 μM. At the end of the incubation, 10 μL of 10% CHAPSO was added to lyse the liposomes to obtain the maximum fluorescence. The data are shown as percentage of maximum fluorescence.

(C) Sulforhodamine B fluorescence at the end of the 60-min incubation shown in (B). Data are presented as the average percentage of maximum fluorescence based on three independent experiments. Error bars indicate SD.

(D) Representative electron micrographs of liposomes incubated with buffer or the indicated peptides. Scale bars, 100 nm.

See also Figure S4.

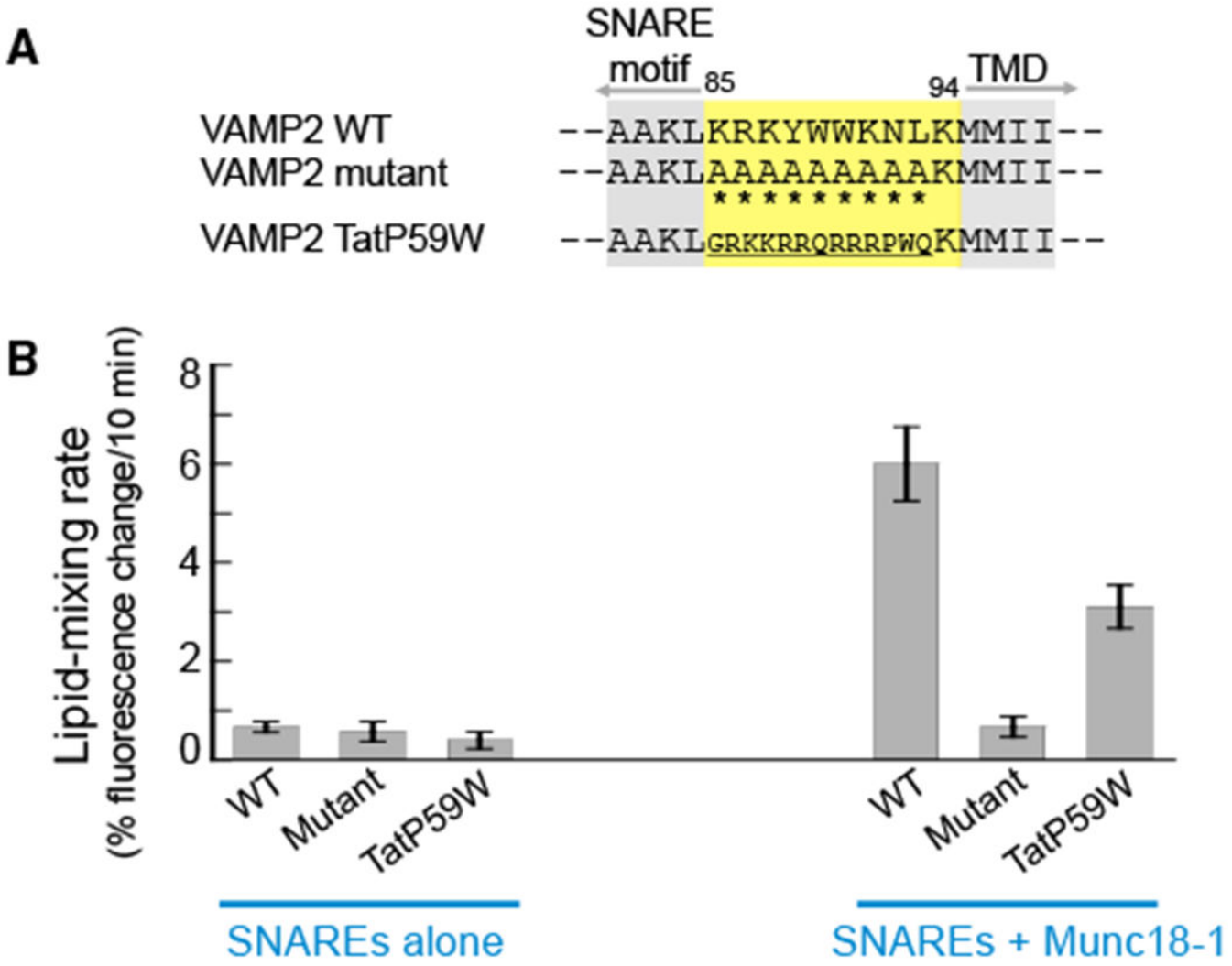

Figure 6. The Juxtamembrane Motif of VAMP2 Can Be Functionally Substituted with an Unrelated Membrane-Destabilizing Peptide

(A) Sequence alignment of the juxtamembrane motifs (highlighted in yellow) of WT and mutant VAMP2 proteins. Asterisks indicate residues mutated into alanines or replaced with the TatP59W peptide. In the VAMP2 TatP59W chimera, the juxtamembrane motif of VAMP2 was replaced with a variant of the HIV-1-derived tat peptide (Thorén et al., 2005). (B) Initial lipid mixing rates of the liposome fusion reactions. WT t-SNARE liposomes were directed to fuse with WT or mutant v-SNARE liposomes in the presence or absence of 5 μM Munc18-1. Data are presented as the average percentage of fluorescence change within the initial 10 min of the reactions based on three independent experiments. Error bars indicate SD.

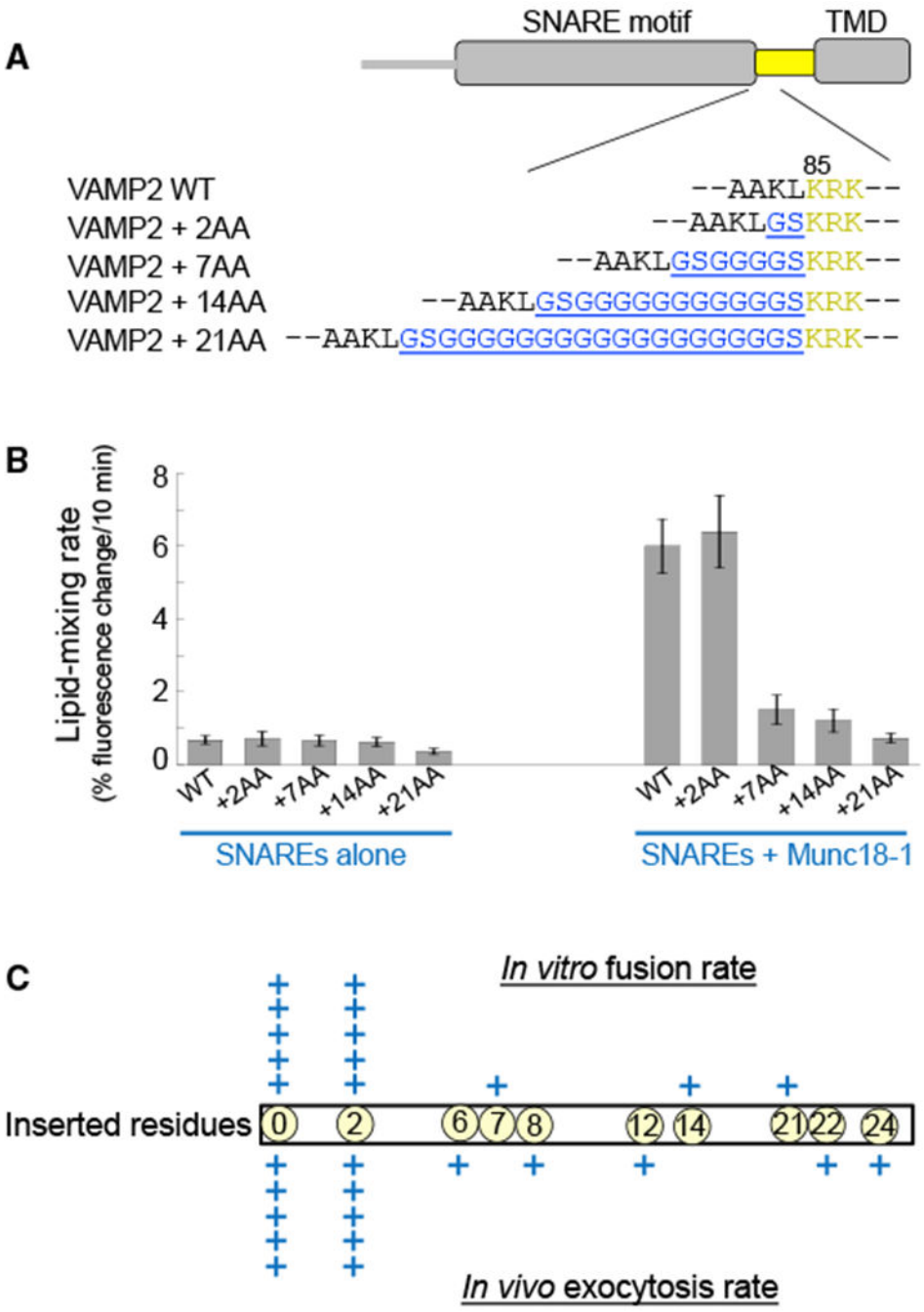

Figure 7. Linker Insertions between the SNARE and Juxtamembrane Motifs Impair Membrane Fusion

(A) Diagram of VAMP2 mutants with insertions of helix-breaking residues (glycines and serines) between the SNARE and juxtamembrane motifs.

(B) Initial lipid mixing rates of the liposome fusion reactions. WT t-SNARE liposomes were directed to fuse with WT or mutant v-SNARE liposomes in the presence or absence of 5 μM Munc18-1. Data are presented as the average percentage of fluorescence change within the initial 10 min of the reactions based on three independent experiments. Error bars indicate SD.

(C) Correlation of the effects of linker insertions on *in vitro* SNARE-Munc18-1-mediated liposome fusion and *in vivo* exocytosis. The *in vivo* data are based on published genetic studies (Deák et al., 2006; Kesavan et al., 2007). The liposome fusion rates were calculated by subtracting the basal level of liposome fusion from SNARE-Munc18-1-mediated liposome fusion. The rates of regulated exocytosis (exocytosis bursts in chromaffin cells or amplitudes of evoked response in cultured neurons) were calculated by subtracting the background levels of exocytosis (in *Vamp2* knockout [KO] cells) from WT cells or *Vamp2* KO cells expressing rescue genes. +++++, 85%–100% of WT levels of liposome fusion or exocytosis; +, <20% of WT levels of liposome fusion or exocytosis.

KEY RESOURCE TABLE

REAGENT or RESOURCE	SOURCE	IDENTIFIER
Antibodies		
Polyclonal anti-Munc18-1	Sigma-Aldrich	Sigma-Aldrich Cat# M2694, RRID: AB_477176
Monoclonal anti-Syntaxin-1	Synaptic Systems	Synaptic Systems Cat# 110 011, RRID: AB_887844
Monoclonal anti-SNAP-25	Synaptic Systems	Synaptic Systems Cat# 111 111, RRID: AB_887792
Monoclonal anti-VAMP2	Synaptic Systems	Synaptic Systems Cat# 104 211, RRID: AB_887811
Bacterial and Virus Strains		
BL21 Gold DE3 competent cells	Stratagene	Cat # 230132
Chemical, Peptides, and Recombinant Proteins		
1-palmitoyl-2-oleoyl-sn-glycero-3-phosphocholine (POPC)	Avanti Polar Lipids	Cat # 850457C
1-palmitoyl-2-oleoyl-sn-glycero-3-phosphoethanolamine (POPE),	Avanti Polar Lipids	Cat # 850757C
1-palmitoyl-2-oleoyl-sn-glycero-3-phosphoserine (POPS)	Avanti Polar Lipids	Cat # 840034C
Cholesterol	Avanti Polar Lipids	Cat # 700000P
N-(7-nitro-2,1,3-benzoxadiazole-4-yl)-1,2-dipalmitoyl phosphatidylethanolamine (NBD-DPPE)	Avanti Polar Lipids	Cat # 810114C
N-(Lissamine rhodamine B sulfonyl)-1,2-dipalmitoyl phosphatidylethanolamine (rhodamine-DPPE)	Avanti Polar Lipids	Cat# 810158C
Nycodenz	Axis-Shield	Cat # 1002424
Sulforhodamine B	Sigma-Aldrich	Cat # 341738
Protease inhibitor cocktail	Roche	Cat # 05056489001
Juxtamembrane motif peptide TSAAKLKRKYWWKNLK	Biomatik	N/A
Recombinant DNA		
pET28a	Novagen	Cat # 69864-3
pGEX4T-3	Addgene	Cat # 27458301
pTW34	Weber et al., 1998	N/A
pET-SUMO-Munc18-1	Shen et al., 2007	Cat # 135550 in Addgene
pET-SUMO-VAMP2	Shen et al., 2007	Cat # 135551 in Addgene
pGEX4T-3-Munc18-1	Shen et al., 2010	N/A
Software and Algorithms		
KaleidaGraph	Synergy	http://www.synergy.com/wordpress_650164087/
ImageJ	NIH	https://imagej.nih.gov/ij/